



This is the author's version of a work that was accepted for publication in the following source:

Perry, D. W. J., Grayden, D. B., Shepherd, R. K., & Fallon, J. B. (2012). A fully implantable rodent neural stimulator. *Journal of neural engineering*, 9(1), 014001.

**Notice:** Changes introduced as a result of publishing processes such as copy-editing and formatting may not be reflected in this document. For a definitive version of this work, please refer to the published source:

The final publication is available at the *Journal of Neural Engineering*:

<http://www.ncbi.nlm.nih.gov/pmc/articles/PMC3373993/>

Copyright of this article belongs to IOP Publishing Ltd, 2012

Published in final edited form as:

*J Neural Eng.* 2012 February ; 9(1): 014001. doi:10.1088/1741-2560/9/1/014001.

## A fully-implantable rodent neural stimulator

DWJ Perry<sup>1,3</sup>, DB Grayden<sup>2,1</sup>, RK Shepherd<sup>1,3</sup>, and JB Fallon<sup>1,3</sup>

JB Fallon: jfallon@bionicsinstitute.org

<sup>1</sup>Bionics Institute, Victoria, Australia

<sup>2</sup>NeuroEngineering Laboratory, Department of Electrical and Electronic Engineering, The University of Melbourne, Victoria, Australia

<sup>3</sup>Department of Otolaryngology, The University of Melbourne, Victoria, Australia

---

The ability to electrically stimulate neural and other excitable tissues in behaving experimental animals is invaluable for both the development of neural prostheses and basic neurological research. We developed a fully-implantable neural stimulator that is able to deliver two channels of intra-cochlear electrical stimulation in the rat. It is powered via a novel omnidirectional inductive link and includes an on-board microcontroller with integrated radio link, programmable current sources, and switching circuitry to generate charge-balanced biphasic stimulation. We tested the implant *in vivo* and were able to elicit both neural and behavioral responses. The implants continued to function for up to five months *in vivo*. While targeted to cochlear stimulation, with appropriate electrode arrays the stimulator is well suited to stimulating other neurons within the peripheral or central nervous systems. Moreover, it includes significant on-board data acquisition and processing capabilities, which could potentially make it a useful platform for telemetry applications, where there is a need to chronically monitor physiological variables in unrestrained animals.

### 1. Introduction

Electrical stimulation of excitable tissue in animal models has numerous applications in basic research, and for studying the safety and efficacy of neural prostheses. Most commonly, electrical stimulation is delivered via a percutaneous connection (e.g. [8]). Whilst this is a simple approach, it is time consuming to maintain the percutaneous wound and there is continual risk of infection migrating along the leadwire. Percutaneous connections are subject to considerable wear (e.g. due to animal grooming) and the external leadwire may impede normal animal behavior. Battery-powered implanted stimulators resolve these issues; however, their lifespan is limited. We developed a stimulator that is fully-implantable, and powered via an omnidirectional inductive link. It is designed to deliver two channels of intra-cochlear electrical stimulation in the rat. The implant builds upon an earlier design developed within our lab [17], addressing several design limitations associated with that device. These include (a) the inability to adjust current level post-implantation (stimulus intensity can only be adjusted by varying pulse width), (b) variable rate of stimulation according to animal orientation, and (c) only single channel stimulation. The improved design addresses all of these issues at the expense of increased complexity and size.

Our design criteria called for the implant to be fully implantable, and have a lifespan of up to six months *in vivo*. The stimulation must be charge-balanced to prevent the non-reversible production of electrochemical byproducts or the delivery of direct current, both of which can lead to tissue damage [20]. The stimulation waveform had to be completely customisable, including pulse width, current and rate, as well as providing the ability to stimulate using complex envelopes, such as amplitude modulation. We required the voltage

compliance to be 5V or more to ensure adequate current could be delivered to the target neural tissue, given a typical electrode impedance of several thousand Ohms. The stimulator had to be compatible with the recording of electrically-evoked potentials to verify neural activation. The implant had a target size of less than 3 cm<sup>3</sup>, although larger implants can be tolerated in rats [18]. The stimulator had to be low maintenance and avoid impeding animal behaviour, which is not always the case for skull mounted connectors (e.g. [27]) or stimulator hardware mounted in a backpack (e.g. [8]). Finally, the implant had to be inexpensive, have minimal requirements for specialized equipment, and be constructed using off-the-shelf components rather than custom silicon. All of these design requirements are met by the implant design described. We now describe the design of the implant, and its performance *in vivo*.

## 1.1. Methods

The implant system (summarized in Figure 1) consists of a plastic animal enclosure, which is wound with three orthogonal coils. Each of these coils is energized in turn, creating a rotating magnetic field. This is inductively coupled to a smaller tuned coil within the implant. This arrangement ensures that power is delivered irrespective of animal orientation. Earlier studies have achieved a similar omnidirectional link by powering each orthogonal coil with a 120° offset between phases [5, 25]. Energy is stored using a small capacitor and regulated to power the microcontroller, radio, and stimulation circuitry. A PC-based controller sends stimulation commands to the implant via a 2.4GHz radio link.

**1.1.1. Implantable Stimulator**—The implant (Figure 1B) consists of a circular four layer circuit board, 17mm in diameter, with a small rectangular stub to which the 2.4GHz antenna was mounted. A coil consisting of 25 turns of enameled copper wire (34G) wound on a ferrite core (3mm diameter, 15mm length, 78 material, Fair-Rite Products Corp.) was coupled with a parallel 122nF capacitor, forming the resonant inductive power receiver. The AC output was rectified by a Schottky diode and limited to 5.6V by a Zener diode. The output was smoothed by a 22μF capacitor and fed into two buck-boost DC-DC power regulators (REG710, Texas Instruments Corp.), outputting 2.7V and 5V, for the control and stimulation circuitry, respectively. A combined microcontroller and 2.4GHz radio transceiver IC (CC2510, Texas Instruments Corp.) was used to communicate with an external PC-based controller, and to control the stimulation circuitry. The stimulation circuitry consisted of three digital SPDT switches (MAX4693, Maxim Corp), which were used to connect the electrodes to the 5V rail or to ground. Two of these outputs were in series with bidirectional current regulators, with the current level set by a digital potentiometer (MAX5493, Maxim Corp). These outputs were capacitively coupled. Unlike a clinical implant, the electrodes were shorted during the inter-phase gap, as the common switch terminal cannot be left floating. This is generally undesirable as it does not serve to reduce current requirements as does a floating inter-phase gap [4, 19]. However, this gap can be skipped or set to a short duration if need be. The combination of capacitive coupling and electrode shorting between stimuli ensures charge balancing [13]. The implant is able to deliver up to 2mA of current at a stimulation rate of up to 600pps. In the current firmware, pulse widths and gaps of up to 255μs can be accommodated. Schematics are shown in the Supplementary Data.

The electrode array used in this study was based on earlier designs used within our lab, constructed using injection molding techniques [21, 26]. It consisted of a platinum banded electrode array within a silastic carrier, 0.31mm in diameter at the tip with 0.45mm between bands. It was connected to the implant using a platinum wire helix within the bulla, followed by a stainless steel helical leadwire. Stimulation was delivered in a bipolar configuration.

**1.1.2. Encapsulation**—Seven implants were constructed and tested in vivo. The first two implants were encapsulated as per [17], using a combination of spray-on silicone conformal coating (DCA SCC3, Electrolube) and silastic (65AR, Permatex). The remaining five implants were protected using a combination of parylene conformal coating and silastic. Parylene is a biocompatible vapour-deposited polymer that provides excellent moisture protection. It is deposited at room temperature. The PCB assemblies were cleaned using a proprietary cleaning solvent (Ultrasolve, Electrolube) in an ultrasonic cleaner until no traces of flux or other contaminants remained when viewed under a microscope. A ball grid array component on the PCB was underfilled with epoxy (U300, Epotek) to prevent any voids in parylene coating. The implants were plasma cleaned for 5 minutes (PlasmaTech, BT1, O<sub>2</sub> plasma, 450W) to remove any remaining contaminants and to improve parylene adhesion. The electrode array was masked off and the assembly coated in Parylene-C (EURO 494, Paratronics Inc.). The stimulator was coated in flowable silastic, with several pieces of silicone sheet (0.127mm, Bioplexus) used as intermediary layers to ensure a minimum coating thickness. The complete implant is shown in Figure 1B.

Polyester mesh (Boston Scientific) was attached to the implant and electrode leadwire to provide a substrate for tissue growth, which aided in securing the implant. During surgery, the polyester mesh was also used to safely grasp the implant and to attach sutures. The implant was kept in saline for at least two weeks for testing, before being rinsed in alcohol and then distilled water, and sterilised using hydrogen peroxide gas plasma (Sterrad, Ethicon Inc).

**1.1.3. Stimulation Enclosure**—The stimulation enclosure (Figure 1C) consisted of a plastic frame, approximately 25×25×25cm in size, as per the design described by [17]. Each of the three orthogonal axes was wound with ten turns of Litz wire (#175/46). The small number of turns allowed animal behaviour to be easily monitored through the walls of the enclosure. Each coil was driven at 500kHz for 1 ms at a time by a Class E amplifier, regulated by a closed loop controller [24]. The RMS current level was set to between 2.7A and 4.2A, depending upon the particular geometry of the coil (i.e. the inner coil required less current than the larger outer coil to produce a similar magnetic flux). Schematics are shown in the Supplementary Data. Because the stimulation waveform is not directly coupled to this omni-directional RF power system, the quality of stimulation does not vary with animal position. Rather, if there is insufficient magnetic flux, the implant stops stimulating altogether. We have provisioned sufficient external coil current to ensure the implant functions reliably during chronic stimulation.

The implant was controlled by a CC2510 development kit (Texas Instruments Corp.) connected to a PC via the serial port. When the implant is powered, it polls the controller at 200ms intervals to check for a new stimulation command. If a new command is available, it is carried out and a verification response is sent to the controller. Radio packets may be lost both to and from the implant, but this arrangement guarantees that the stimulation command is carried out. Occasionally, the verification response from the implant is lost and so stimulation is repeated. A fan was mounted above the enclosure to ensure adequate ventilation. A photo of the stimulation enclosure, coil driver and controller are shown in the Supplementary Data. The strength of the magnetic field was measured (MC162; Magnetic Sciences) at 500kHz, and was found to meet occupational and public exposure guidelines, provided a 1m clearance was maintained while the coils were energized [14].

**1.1.4. Surgery**—Animal trials were approved by the St. Vincent's Hospital Animal Research Ethics Committee (#07/149). The stimulators were implanted in seven adult rats (Hooded Wistar, >12w old) using surgical procedures as described previously [16, 17]. Briefly, the animal was anesthetized using isoflurane in oxygen (1-2%) and a sub-auricular

incision made to access the bulla. The bulla was opened and stapedial artery cauterized around the round window using bipolar coagulation. A cochleostomy was made adjacent to the round window, and the electrode array inserted into the scala tympani. The cochleostomy was sealed with a muscle plug and the bulla filled with dental cement to secure the electrode array. Figure 3 gives an overview of the implanted components. The leadwire was fixed at the skull using a polyester mesh tie, and the implant and leadwire threaded into a subcutaneous pocket along the back. The wounds were closed in two layers using sutures and skin staples. Prophylactic antibiotics and analgesia were administered for three days.

**1.1.5. Evoked Potential Recording**—The electrically-evoked auditory brainstem response (EABR) measures activation of the ascending auditory pathway in response to electrical stimulation of the auditory nerve. It is useful to record the EABR in chronically implanted animals so that implant functionality can be verified, and an appropriate chronic stimulation level set.

EABRs were recorded as described previously [17, 23]. Briefly, the animals were anesthetized using a ketamine/xylazine mixture (70/6.5 mg/kg) during recording sessions. The EABR was scalp recorded using needle electrodes at the vertex and neck. A ground electrode was inserted at the nose, which avoids interference from the stimulator's RF power system. The recording electrodes were connected to an amplifier (ISO-80, WPI Instruments) with 100× gain, and bandpass filtered between 5Hz and 10kHz. The output was connected to a data acquisition system (NI USB-6251, National Instruments) driven by a PC. A stimulation command was sent to the implant, which selected the stimulus rate (30pps), pulse width (50μs), current (0 to 2000μA in 100μA steps) and number of pulse repetitions (100). The raw recording was then analysed by custom software, using the stimulus artifact time (detected by a simple level crossing) to generate a raw averaged response. This allowed identification of the stimulus timing at current levels down to 200μA for bipolar stimulation. This approach may prevent the determination of very low thresholds, although pulse width can be reduced as required to ensure that at least one sub-threshold response can be recorded. This averaged response was bandpass filtered between 300 and 3000Hz to obtain the EABR at each current level.

The chronic stimulation enclosure generates a 333Hz magnetic field as the field orientation is switched, which would interfere with EABR recordings. To overcome this, a single coil was used to power the implant during EABR sessions. The coil was identical to that on the implant, and was driven by a simple circuit consisting of a sine wave generator and high current op-amp. It was placed parallel to the receiving coil, and could power the implant at a distance of 5mm, which was sufficient to penetrate the skin.

In a separate acute study in one animal, we recorded EABRs using both the implanted stimulator and our standard benchtop laboratory stimulator, developed in-house, connecting each as required using a percutaneous connector. A diagram detailing the EABR recording procedure for both acute and chronic experiments is shown in the supplementary data section.

**1.1.6. Chronic Stimulation**—Chronic stimulation was performed in three animals once they had recovered from surgery, and an EABR was able to be recorded. The chronic stimulation program consisted of amplitude modulated pulse trains (bipolar, 50μs pulse width, 10μs inter-phase gap, 300pps rate) between 5 and 150Hz at 100% depth, for four hours a day, five days a week. Current level was set at 100μA above EABR threshold. Chronic stimulation was ceased if the implant or electrode array failed (i.e. lack of radio contact or if no electrical artifact or EABR could be recorded).

## 1.2. Results

An example output pulse train from one stimulation channel is shown in Figure 2 using a 1k $\Omega$  load. It demonstrates that current level can be dynamically varied, unlike the earlier design developed in our lab where current level is fixed post-implantation, and stimulus intensity can only be adjusted by varying pulse width [17]. Further output waveforms are included in the Supplementary Data, using a larger 5.6k $\Omega$  load, as well as an intra-cochlear electrode array placed in saline.

The results of *in vivo* testing are summarized in Table 1. The first two stimulators (#1,2), encapsulated using a spray-on silicone conformal coating, failed after approximately one month post-implantation due to fluid ingress. While we were able to elicit a behavioral response, we failed to record an EABR prior to implant failure. Examination of the stimulator revealed corrosion where the leadwire was soldered to the PCB assembly, suggesting the conformal coating (which was not heat cured at the electrode connections) had failed. The electrode array was intact, and when percutaneously connected to a laboratory stimulator, an EABR was able to be recorded.

Three of the five subsequent implants, protected using Parylene, withstood chronic implantation, and functioned normally. A further implant (#5) functioned intermittently while implanted. This was likely due to an increased tissue response associated with an inflammatory response. The implant functioned normally upon explantation. The final implant (#7) was not able to be contacted immediately after implantation, although upon explantation and drying, the implant functioned normally. Microscopic examination revealed no obvious corrosion, suggesting partial fluid ingress. Whilst the parylene appeared intact in all implants, the outer siliastic was readily removed, indicating poor adhesion to the parylene.

The electrode array failed in all but three animals, typically after at least two weeks. This was apparent through the lack of an EABR, electrical artifact, and high electrode impedance upon explantation. Examination of the electrode array showed that all failures could be attributed to breakage at the connection between the stainless steel and platinum wires. Stimulation waveforms were inspected in working implants upon explantation and were not found to differ to those produced prior to implantation (Figure 2).

Figure 4 shows a comparison of EABRs recorded acutely in one animal using stimulation generated by the implanted or laboratory stimulator. The response amplitude, latency and threshold (700 $\mu$ A) are nearly identical over the 100 $\mu$ A current steps used. We were able to record an EABR in three chronically implanted animals at two weeks post implantation. A further EABR was recorded in one animal six weeks post implantation. While threshold increased in this second recording, this cannot be simply attributed to stimulator performance, as threshold may increase due to tissue encapsulation of the electrode array, or changes in the peripheral and central nervous system following deafness and chronic stimulation (e.g. [6, 10]).

In animals where an EABR was recorded, there was a clear behavioral response to the first suprathreshold stimulus, at a level equal to or below EABR threshold. The animals quickly habituated to the stimulation, and showed little or no response to subsequent stimulation. Chronic stimulation was well-tolerated, with no deleterious effects (e.g. weight loss) from either the stimulation or magnetic field observed.

## 1.3. Discussion

We developed a novel fully-implantable neural stimulator, fabricated using off-the-shelf components, powered via an omni-directional wireless link. It was implanted in seven

animals and successfully stimulated the auditory nerve for periods of up to five months. A separate acute study demonstrated that the neural activation produced by our implant was indistinguishable from that produced by an existing neural stimulator. This demonstrates that the implant is successfully stimulating the auditory nerve and is equivalent to established stimulation procedures used in our laboratory.

The first two implants encapsulated using a silicone conformal coating failed after one month. An earlier implant design [17] utilizing this method proved reliable, ostensibly because critical components were located some distance from the non-heat cured leadwire connections. In contrast, the current implant design places components only millimeters away, such that ingress fluid may readily short the power supply. We tested a fully heat cured implant in saline at 37°C (data not presented); it continued to function normally for six months. Heat curing was not applied to the entire implant due to the fragility of the electrode array, although in retrospect we found that this introduced a failure site in our stimulator. Parylene coating, which may be applied to the entire implant at room temperature, was used in later implants. This proved reliable in four out of five implants. Parylene has a long history as an encapsulation material, and under ideal conditions may be expected to last a year or more [11, 12, 15, 22]. Implants that failed did so completely (i.e. we could not contact them by radio to initiate stimulation). We found no evidence that the quality of stimulation varies over time.

While not related to the stimulator design described herein, the electrode array proved to be the most troublesome aspect of *in vivo* testing, eventually failing in four of seven animals. The weak point appears to be the connector between the platinum and stainless steel wires. This issue may be resolved by constructing the electrode array and leadwire from a single length of platinum, eliminating the connector. This is the approach taken in our mouse implant design [17].

The microcontroller on the implant contains several analog to digital channels, and combined with additional amplification, buffering and storage circuitry on a second PCB, may be used to monitor electrode impedance, or record neural or other physiological responses. A small rechargeable battery could be added to allow telemetry or stimulation in any environment, with the stimulation enclosure used only for charging [3]. The maximum pulse width is limited to 255 $\mu$ s by the current firmware, however this can be easily modified to allow for longer pulse widths. While the implant does not contain a DSP, the microcontroller has sufficient processing power to permit simple event analysis and potentially form a closed loop neural prosthesis for use in animal studies. With the addition of an appropriate electrode array, it could be used in animal studies of deep brain, motor and sensory stimulation, both for development and safety studies. It may also find utility in basic neuroscience research, where chronic electrical stimulation needs to be delivered to unrestrained behaving animals. While the stimulator system can be readily adapted to larger animals, it is unlikely to be tolerated by smaller species, such as mice, without first integrating much of the circuitry into an application specific integrated circuit to reduce the stimulator volume.

The implantable stimulator described by Winter et al [25] most closely resembles our own. It similarly used a rotating magnetic field (at 82kHz), combined with a separate FM transmitter (at 140MHz), to provide stimulation in freely-behaving animals. It is slightly larger than our implant, and while it can generate arbitrary stimulation waveforms, it is limited to a single stimulation channel. Several commercially-available telemeters share characteristics with our stimulator, namely that they are fully-implantable, have a long life-span, and don't restrain animal behavior [3, 7]. In particular, the design described by Budgett et al [3], where a battery-powered implant is able to be repeatedly charged using an

inductive charging platform, placed under the animal's enclosure, could be redesigned to deliver electrical stimulation. Several other wireless neural stimulators have been published, but they either require custom silicon, batteries, or are not fully implantable (e.g. [1, 2, 9, 27]).

Where neural stimulation studies require only fixed, constant current stimulation, the simpler stimulator developed previously by our lab would prove appropriate [17, 23]. This stimulator is smaller, has far fewer components, and therefore less potential failure modes. However, if precise control over the stimulus waveform or multiple channels are required, then the stimulator described here would prove useful. Whilst only AM stimulation is implemented in the current implant firmware, it can readily store and deliver other arbitrary stimulation waveforms, varying pulse width, current, timing and channel on the fly. The stimulator design described is presently being used to examine the effects of chronic AM cochlear stimulation on the rat auditory cortex, a study that would not be possible with our earlier implant design.

## Supplementary Material

Refer to Web version on PubMed Central for supplementary material.

## Acknowledgments

We thank Rodney Millard, Ben Wei, Jin Xu, Ricki Minter, Hugh McDermott and Helen Feng for their contribution, and Sue Peirce, Elisa Borg and staff at the BRC for providing exceptional animal care. Minifab Pty. Ltd. provided parylene coating services for which we are very grateful. This work was funded by NIDCD (HHS-N-263-2007-00053-C). The Bionics Institute acknowledges the support it receives from the Victorian Government through its Operational Infrastructure Support Program.

## References

1. Arfin SK, Long MA, Fee MS, Sarpeshkar R. *J Neurophysiol.* 2009; 102(1):598–605. [PubMed: 19386759]
2. Ativanichayaphong T, He JW, Hagains CE, Peng YB, Chiao JC. *J Neurosci Methods.* 2008; 170(1): 25–34. [PubMed: 18262282]
3. Budgett DM, Hu AP, Si P, Pallas WT, Donnelly MG, Broad JWT, Barret CJ, Guild SJ, Malpas SC. *J Appl Physiol.* 2007; 102:6.
4. Carlyon RP, van Wieringen A, Deeks JM, Long CJ, Lyzenga J, Wouters J. *Hear Res.* 2005; 205(1-2):210–24. [PubMed: 15953530]
5. Cools AR, Lambrechts P, van Bommel J. *Med Biol Eng Comput.* 1978; 16(5):559–563. [PubMed: 102882]
6. de Sauvage RC, da Costa DL, Erre JP, Aran JM. *Hearing Research.* 110:119–134. [PubMed: 9282894]
7. E-Mitter Battery-Free Implantable Transponders n.d. URL <http://www.minimitter.com/emitter.cfm>
8. Fallon JB, Irvine DRF, Shepherd RK. *J Comp Neurol.* 2009; 512(1):101–114. [PubMed: 18972570]
9. Ghovanloo M, Najafi K. *IEEE Trans Neural Syst Rehabil Eng.* 2007; 15(3):449–457. [PubMed: 17894278]
10. Hardie NA, Shepherd RK. *Hear Res.* 128(1-2):147–65. [PubMed: 10082295]
11. Hassler C, von Metzen RP, Ruther P, Stieglitz T. *J Biomed Mater Res B Appl Biomater.* 2010; 93(1):266–274. [PubMed: 20119944]
12. Hsu JM, Rieth L, Normann RA, Tathireddy P, Solzbacher F. *IEEE Trans Biomed Eng.* 2009; 56(1):23–29. [PubMed: 19224715]
13. Huang CQ, Shepherd RK, Carter PM, Seligman PM, Tabor B. *IEEE Trans Biomed Eng.* 1999; 46(4):461–70. [PubMed: 10217884]

14. International Commission on Non-Ionizing Radiation Protection. *Health Phys.* 1998; 74(4):494–522. [PubMed: 9525427]
15. Loeb GE, Bak MJ, Salcman M, Schmidt EM. *IEEE Trans Biomed Eng.* 1977; 24(2):121–128. [PubMed: 408260]
16. LU W, Xu J, Shepherd RK. *Hear Res.* 2005; 205(1-2):115–22. [PubMed: 15953521]
17. Millard RE, Shepherd RK. *J Neurosci Methods.* 2007; 166(2):9.
18. Moran MM, Roy RR, Wade CE, Corbin BJ, Grindeland RE. *J Appl Physiol.* 1998; 85(4):1564–71. [PubMed: 9760354]
19. Prado-Guitierrez P, Fewster LM, Heasman JM, McKay CM, Shepherd RK. *Hear Res.* 2006; 215(1-2):47–55. [PubMed: 16644157]
20. Shepherd, RK.; Meltzer, NE.; Fallon, JB.; Ryugo, DK. chapter Consequences of deafness and electrical stimulation on the peripheral and central auditory system. 2nd. Thieme Medical Publishers, Inc; New York: 2006. p. 25-39.
21. Shepherd RK, Xu J. *Hear Res.* 2002; 172(1-2):92–8. [PubMed: 12361871]
22. Stieglitz T, Haberer W, Lau C, Goertz M. *Conf Proc IEEE Eng Med Biol Soc.* 2004; 6:4178–4181. [PubMed: 17271224]
23. Tan J, Widjaja S, Shepherd RK. *Cereb Cortex.* 2008; 18(8):1799–1813. [PubMed: 18063565]
24. Troyk PR, Schwan MA. *IEEE Trans Biomed Eng.* 1992; 39(6):589–99. [PubMed: 1601440]
25. Winter KF, Hartmann R, Klinke R. *J Neurosci Methods.* 1998; 79(1):79–85. [PubMed: 9531463]
26. Xu J, Shepherd RK, Millard RE, Clark GM. *Hear Res.* 105(1-2):1–29. [PubMed: 9083801]
27. Zhang Y, Langford B, Kozhevnikov A. *J Neurosci Methods.* 2011; 202(1):1–8. [PubMed: 21903132]

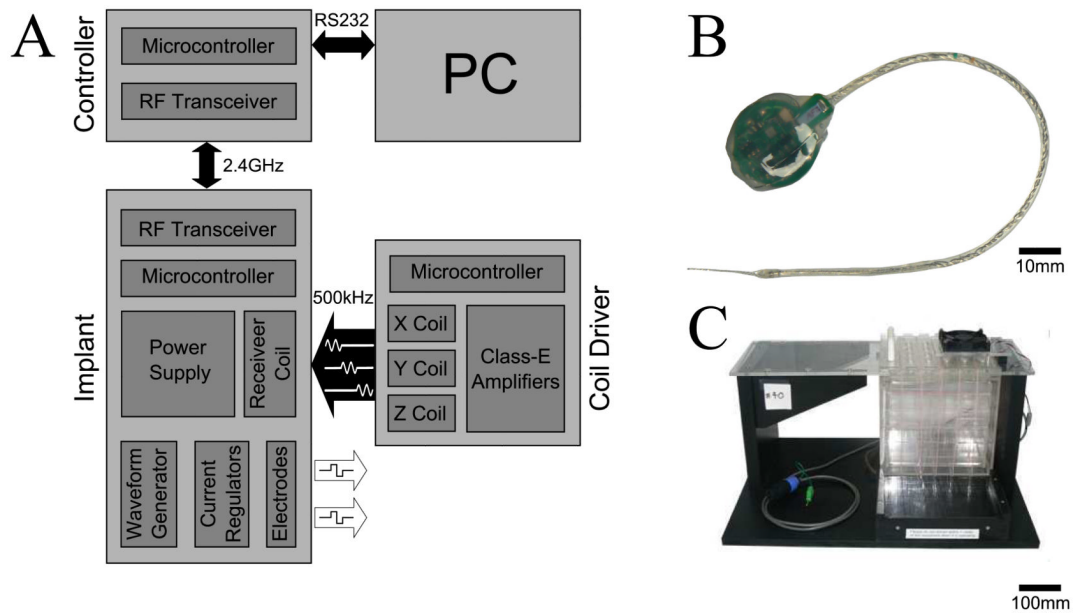


**Figure 1.** (A) Block diagram of implant system, consisting of implanted stimulator, wireless power delivery and controller. (B) Photo of implant, prior to attachment of polyester mesh. (C) Photo of stimulation enclosure, without controller.

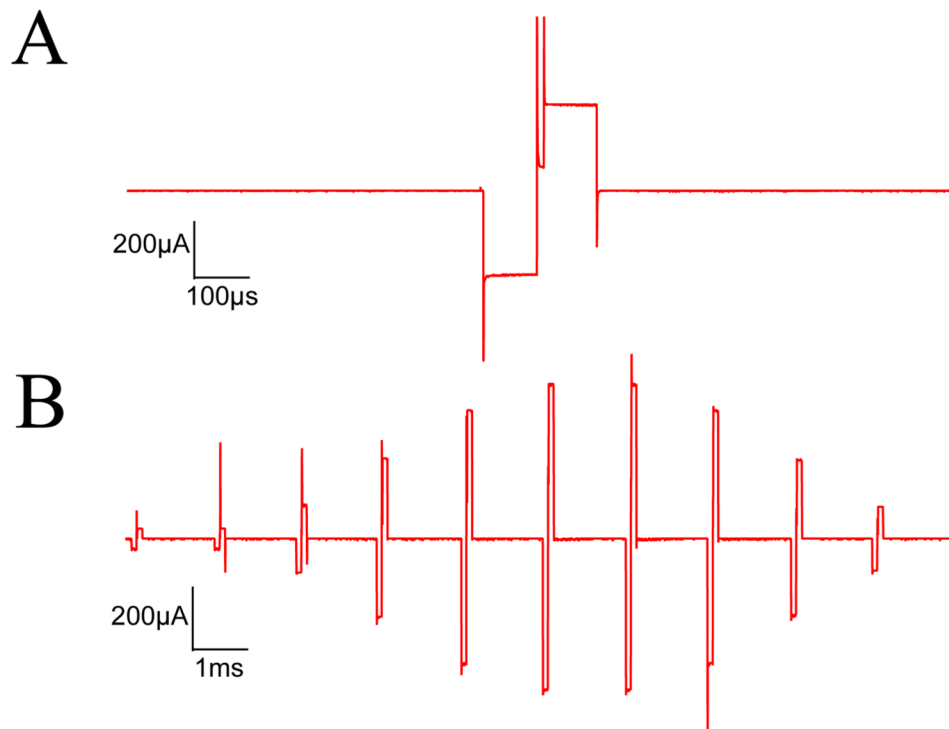


**Figure 2.** Example of AM stimulus output (600pps,  $f_m=60\text{Hz}$ , depth=100%, 100 $\mu\text{s}$  pulse width, 10 $\mu\text{s}$  inter-phase gap, 1k $\Omega$  load, 600 $\mu\text{A}$  peak current). (A) Detail of a single pulse (B) A 20ms segment of the AM pulse train. The current spikes at the pulse onsets are over-emphasized by the oscilloscope sampling, and are minimal when driving a reactive biological load.

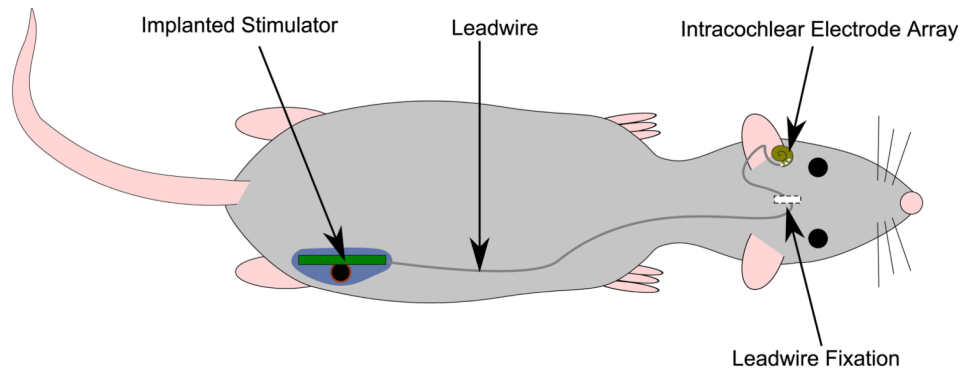


**Figure 3.** Overview of implanted components, showing intracochlear electrode array, fixation at the skull (using polyester mesh), leadwire, and stimulator.

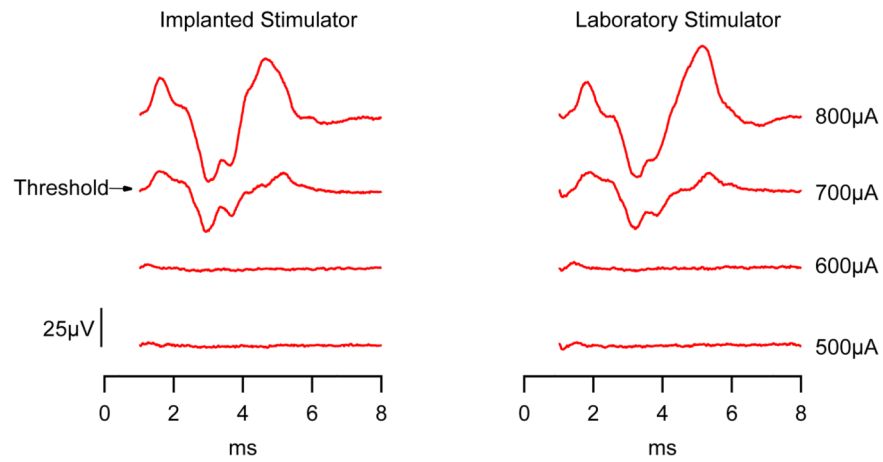


**Figure 4.**

Comparison of EABRs produced by a fully implanted stimulator (left) versus a laboratory based stimulator (right), using a bipolar stimulus with  $25\mu\text{s}$  pulse width, and  $10\mu\text{s}$  inter-phase gap, averaged over 100 pulses delivered at 30pps. The first 1ms of the response was blanked to remove any stimulus artifact.

Tabular summary of *in vivo* results, including EABR threshold (at 2 and 6 weeks post-implantation, if available) and whether the stimulator and electrode array were functional upon explantation. Details of suspected failure mechanisms for each implant are described in the main text.

**Table 1**

Implant	Encapsulation	Implant Time (days)	EABR Threshold ( $\mu$ A)	Stimulator	Electrode
1	Silicone	48	N/A	✗	✓
2	Silicone	44	N/A	✗	✓
3	Parylene	54	500/700	✓	✓
4	Parylene	152	300	✓	✗
5	Parylene	77	600	✓	✗
6	Parylene	75	N/A	✓	✗
7	Parylene	33	N/A	✗	✗